

Recent Progress in Dye-Sensitized Solar Cells Using Nanocrystallite Aggregates

Qifeng Zhang,* Kwangsuk Park, Junting Xi, Daniel Myers, and Guozhong Cao*

Nanocrystallite aggregates are spherical assemblies of nanometer-sized crystallites and feature a size on the order of sub-micrometers. This paper reports and summarizes recent progress in nanocrystallite aggregates for applications in dye-sensitized solar cells. It emphasizes that nanocrystallite aggregates are a promising class of materials with the capability to generate light scattering, enhance electron transport, retain high specific surface area for dye adsorption, and facilitate electrolyte diffusion while serving as the photoelectrode film of a dye-sensitized solar cell. In the *Perspectives* section, it is suggested that optimization of the porosity of the aggregates, the facets of nanocrystallites forming the aggregates, and the structure of photoelectrode film could possibly lead to breakthroughs in improving the power conversion efficiency of the current state-of-the-art dye-sensitized solar cells.

1. Introduction

Dye-sensitized solar cells (DSCs) are a type of photovoltaic device based on the charge transfer process between dye molecules and an oxide.^[1–5] The oxide is usually in the form of a nanostructure, providing a large surface area for chemical adsorption of the dye molecules.^[6–8] The dye molecules, serving as the sensitizer of the solar cell, are designed to be able to absorb light in solar spectrum in order to generate photoexcited electrons. The photoexcited electrons then transfer to the oxide and form a conduction current through an external circuit. A liquid electrolyte, typically containing I^-/I_3^- redox couples, is employed in DSCs to conduct the electrons injected from the counter electrode, which is connected to the photoelectrode through the external circuit, to reduce the dye molecules that are oxidized by photoexcitation. DSCs offer several advantages over silicon-based p-n junction solar cells, including lower cost in both materials and manufacturing and compatibility with flexible substrates. While polymer-based solar cells are also compatible with flexible substrates, DSCs currently demonstrate higher conversion efficiencies, better chemical stability, and longer operating lifetimes compared to polymer-based solar cells.

DSCs have undergone two decades of development since they were invented in 1991.^[9] At that time, an initial 7.1%

efficiency was announced. Relying on progressive optimization in device structure and the advent of highly efficient metal-organic dyes, the efficiency record of DSCs has recently reached 11–12%.^[10,11] Typical metal-organic dyes are a class of polypyridyl complexes of ruthenium, such as N3,^[12] N719,^[11,13] and “black dye”.^[14] These dyes are already commercially available. Other dyes derived from the ruthenium complexes, including K19,^[15,16] C101,^[17] and K8,^[18] have also been reported to have high efficiencies of around 10–11%.^[19] As the “antenna” of the DSC for light harvesting, the dye is one of the most important components, determining the overall conversion efficiency of the cell. If the

dye absorption edge is extended from the current 800–850 nm to 920–940 nm, it has been predicted that the efficiencies of DSCs would be further increased, perhaps reaching as high as 14–20%.^[20–22]

Aside from the dye sensitizer, another critically important component of DSCs is the nanostructured oxide film. On one hand, the oxide film acts as a “backbone” to hold the dye molecules, and therefore the structure of the oxide film (i.e., the porosity, or internal surface area) affects the amount of dye adsorbed by the photoelectrode. On the other hand, the oxide film provides pathways for electron transport, and accordingly both the electron transport and the ion diffusion in the electrolyte may be affected by the film structure. Charge recombination, resulting from a reaction between the photoexcited electrons and oxidized electrolyte species, is a phenomenon existing in DSCs concerning the transport of photoexcited electrons and therefore is related to the structure of the oxide film.^[23] Charge recombination adversely affects the performance of the cell. Recombination is particularly serious in the case of photoelectrodes consisting of a nanocrystalline oxide film. This is because the film of nanocrystallites (or nanoparticles; these two terms are used interchangeably in this paper), while providing a large internal surface area for dye adsorption, also results in a large interface for the photoexcited electrons in the oxide to recombine with the oxidized ions in electrolyte.

Besides the charge recombination effect, the numerous boundaries between nanocrystallites is another drawback of nanocrystalline films. Such boundaries may trap photoexcited electrons and therefore diminish the electron transport within the photoelectrode film. One-dimensional nanostructures, such as nanowire and nanotube arrays of ZnO or TiO₂, have been intensively studied for application to DSCs with the aim

Prof. Q. F. Zhang, K. Park, J. T. Xi, D. Myers, Prof. G. Z. Cao
Department of Materials Science and Engineering
University of Washington
Seattle, WA 98195, USA
E-mail: qfzhang@u.washington.edu; gzcao@u.washington.edu

DOI: 10.1002/aenm.201100352

of providing direct pathways for electron transport to reduce charge recombination.^[24] However, when compared with the nanoparticles, one-dimensional nanostructures present insufficient internal surface area for dye adsorption and therefore yield relatively low efficiencies. For example, a photoelectrode film composed of 20 μm -long TiO_2 nanotube arrays demonstrated an efficiency of 6.89%,^[25] which was significantly lower than the 10–11% efficiencies for nanocrystalline films with thicknesses of several tens of micrometers. It is worth noting that the 20 μm thickness of the photoelectrode film is reasonable since the effective diffusion length of photoexcited electrons in photoelectrode films composed of one-dimensional nanostructures is significantly longer than that in a nanocrystalline film; for latter, it is typically below ten micrometers.^[5,26]

This paper reports recent progress in development of DSCs with photoelectrode films employing a new nanostructure, the so-called oxide nanocrystallite aggregates. An important feature of this nanostructure is that it not only possesses a large surface area resulting from using nanometer-sized crystallites as the building unit, but also presents other benefits such as: 1) improving optical absorption via generation of light scattering; 2) enhancing electron transport owing to a compact structure of nanocrystallites within the aggregates; and 3) facilitating the diffusion of ions in electrolyte through large pores in the photoelectrode film consisting of spherical aggregates.^[27] One successful example of using nanocrystallite aggregates for DSCs is that photoelectrode films composed of ZnO nanocrystallite aggregates have shown a more than twofold increase in overall conversion efficiency compared with films composed of dispersed ZnO nanoparticles.^[28,29] Similar studies have been also carried out on TiO_2 . For example, the so-called mesoporous TiO_2 spheres or beads achieved efficiencies over 10%,^[30] comparable to the certified efficiency record for conventional DSCs constructed with nanocrystalline films. In the *Perspectives* section, several routes are proposed towards improving the performance of DSCs using nanocrystallite aggregates. It emphasizes that the TiO_2 nanocrystallite aggregates are a promising material that may lead to a breakthrough in the conversion efficiency of the current DSCs.

2. Conventional DSCs Based on Nanocrystalline Films

Conventional DSCs are based on TiO_2 nanocrystalline films sensitized with polypyridyl ruthenium complexes, such as N3, N719, or “black dye”, as the dye.^[31–33] The dye molecules, which adsorb on the oxide in a monolayer, are functionalized to harvest light and then inject the photogenerated electrons into the oxide. The nanoparticles that comprise the photoelectrode film are typically ~15–20 nm in diameter, yielding a specific surface area of ~100 m^2/g , which has been demonstrated to be ~1000-fold larger than that of a flat film.^[9] Over the past two decades, conventional DSCs have undergone development from a single layer structure to a double layer structure; the latter employs large TiO_2 particles (~400 nm in diameter) applied on the top of nanocrystalline film to generate light scattering/reflection so as to enhance the optical absorption of the photoelectrode. At the same time, the dyes have been also intensively developed, with attention paid to increasing



Qifeng Zhang, Ph.D., is currently working at University of Washington as a Research Assistant Professor. His research interests involve engineering applications of nano-structured materials on electrical devices including solar cells, UV light-emitting diodes (LEDs), field-effect transistors (FETs), and gas sensors. His current research

focuses on the synthesis of nanomaterials and the application of nanomaterials in electronic and optoelectronic devices such as dye-sensitized solar cells (DSCs) and organic/inorganic hybrid solar cells.



Guozhong Cao, Ph.D., is the Boeing-Steiner Professor of Materials Science and Engineering and Adjunct Professor of Chemical and Mechanical Engineering at the University of Washington. He has published over 250 refereed papers, and authored and edited 5 books including “Nanostructures and Nanomaterials”. His

current research is focused mainly on nanomaterials for energy conversion and storage including solar cells, lithium-ion batteries, supercapacitors, and hydrogen storage materials.

the extinction coefficient and/or extending the absorption edge toward the near-infrared region of the solar spectrum.^[34]

2.1. Single Layer Structure

The first reported DSCs included a photoelectrode film constructed with a single layer of TiO_2 nanocrystallites sensitized by a trimeric ruthenium complex known as N3 dye.^[9] The film was ~10 μm in thickness and the average size of the nanocrystallites was 15 nm. The 7.1% efficiency achieved at that time was significantly higher than those efficiencies (typically below 1%) obtained for other previously reported systems. The attainment of high efficiency was first of all attributed to the porous structure of the photoelectrode film which consisted of nanocrystallites forming a three-dimensional network that provided an extremely large surface for dye adsorption. The internal surface area of such a photoelectrode film was estimated to be 780 cm^2 for each 1 cm^2 of geometric surface, almost three orders of magnitude larger than that of a flat film. Another important factor leading to such high efficiency was the newly developed N3 dye, which possessed a large extinction coefficient ($1.3 \times 10^4 \text{ M}^{-1} \text{ cm}^{-1}$ at

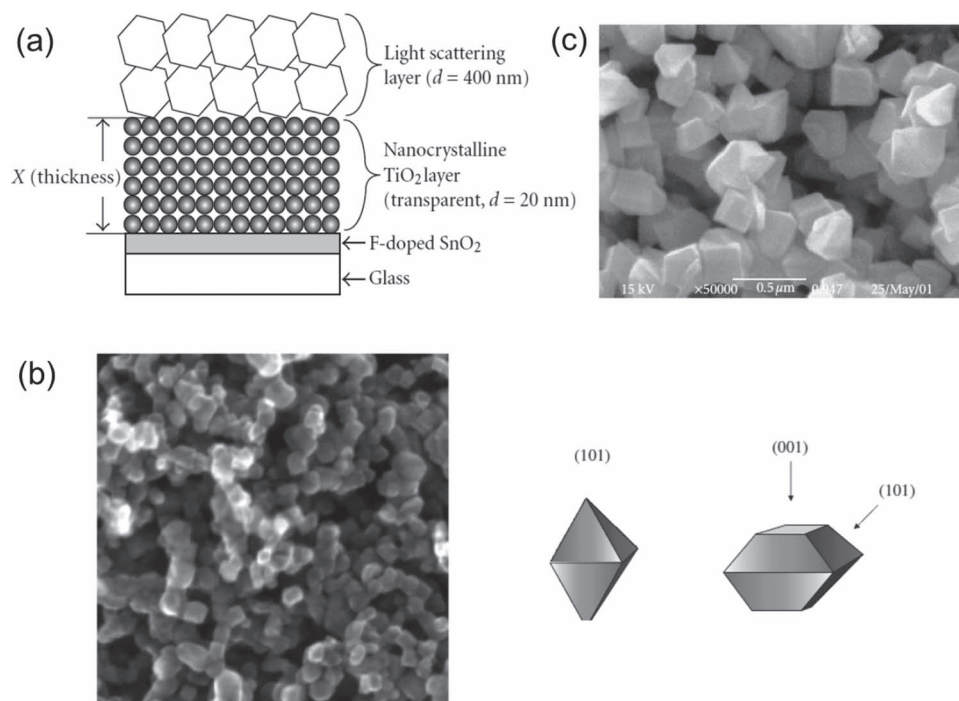


Figure 1. Double layer structured photoelectrode in DSCs. (a) Schematic drawing of double layer structure, (b) SEM image of anatase TiO_2 nanocrystallites averagely 20 nm in diameter with mainly exposed (101) facet followed by (100) and (001) orientations, and (c) SEM image of 400-nm large particles of TiO_2 (400C, JGC-CCIC) as light scatterers. Reproduced with permission.^[5,35,36] [5] Copyright 2005, American Chemical Society. [35] Copyright 2009, Hindawi Publishing Corporation. [36] Copyright 2005, Chemical Society of Japan.

518 nm wavelength) and greatly extended the absorption onset to the near-infrared region of the solar spectrum at ~ 750 nm wavelength. This dye adsorbed to form a monolayer on the TiO_2 and efficiently injected the photogenerated electrons into the TiO_2 through a metal-to-ligand charge transfer (MLCT) process.^[3] In general, the combination of TiO_2 nanoparticles and ruthenium complex dye delivered an ideal system that could simultaneously satisfy the requirements of: 1) a large surface area of oxide to allow for chemical adsorption of dye molecules; and 2) suitable relative energy levels between the dye and the oxide enabling highly efficient electron injection. The efficiency was improved to $\sim 10\%$ in 1993 by increasing the film thickness to $\sim 12 \mu\text{m}$, modifying the surface of the nanocrystalline film using TiCl_4 , and optimizing the electrolyte.^[12] Other types of ruthenium dyes were subsequently developed, typically including N719 (in 1999) which provided a higher open-circuit voltage than N3, and “black dye (i.e., N749)” (in 2001) which extended the light absorption onset to 860 nm. These dyes further improved the performance of DSCs to a maximum conversion efficiency of $\sim 10.4\%$ when used with a photoelectrode film 18 μm in thickness.^[14]

2.2. Double Layer Structure

Nanocrystallites serving as a photoelectrode film can provide a large surface area. However, one of the drawbacks of nanocrystalline films is that the size of the nanocrystallites is far smaller than the wavelengths of visible light, and therefore, a photoelectrode film composed of nanocrystallites is transparent to

visible light. Thus, the thickness of the photoelectrode film is required to be greater than the optical absorption length ($1/\alpha$) to enable sufficient absorption of incident light, particularly at wavelengths deviating from the absorption peaks of the dye. However, the thickness of the photoelectrode film of a DSC is also limited by the diffusion length (L_n) of photogenerated electrons in the nanocrystalline film, arising from the existence of electron trapping sites and charge recombination during the transport of electrons. The deficiency of nanocrystalline films in optical absorption arising from electron transport restrictions on thickness can be compensated for to some degree by adopting a double layer structure. The double layer structure includes a nanocrystalline film as the primary absorption layer and a top layer of large TiO_2 particles (~ 400 nm in diameter) for light scattering (Figure 1).^[35,37] With such a double layer structure, the incident light can be reflected back to the nanocrystalline film by the scattering layer, thus extending the traveling distance of light within the photoelectrode film so as to increase the probability of interaction occurring between the photons and the dye molecules.^[38] It is widely accepted that the use of double layer structure in DSCs is an effective way to significantly enhance the optical absorption of the photoelectrode, especially in the near-infrared region with wavelengths over 700 nm where the dye is not as efficient at absorbing light.^[39]

2.3. Mixture Structure

The mixture structure is another binary architecture applied to DSC photoelectrode. In the mixture structure, large particles

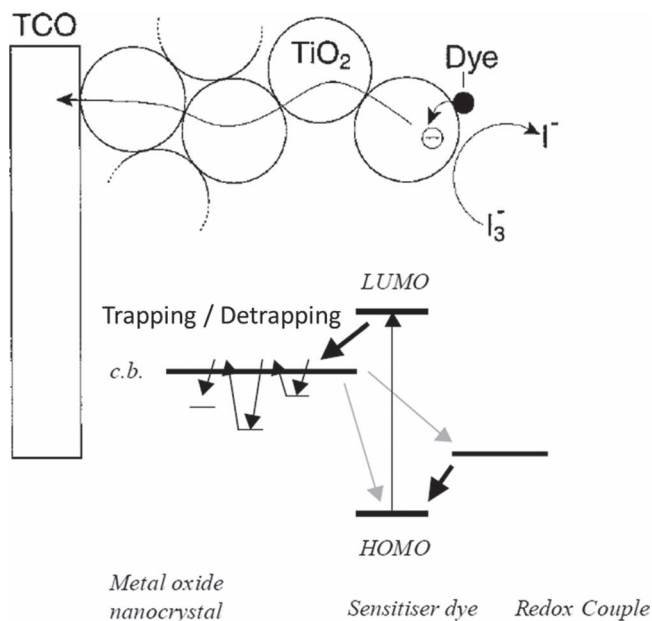


Figure 2. Charge recombination and electron trapping/detrapping in DSCs.^[23,42] [23] Copyright 2004, Elsevier B.V.. [42] Copyright 2000, American Chemical Society.

are embedded into the nanocrystalline film to act as light scatterers. The use of a mixture structure has increased the conversion efficiency to ~10% from the initial ~7.1% for films sensitized with N3 dye.^[40]

2.4. Problems Existing in Conventional DSCs

2.4.1. High Recombination Rate and Electron Trapping

In DSCs, charge recombination arising from reactions between the photogenerated electrons and the oxidized electrolyte species (I₃⁻) is the predominant mechanism of energy loss.^[41] The recombination is particularly serious in the case of photoelectrode films comprising nanocrystallites because nanocrystallites, with a size on the order of several tens of nanometers, soaked in a liquid electrolyte with high ion concentration cannot support a potential gradient for the separation of photogenerated charges or facilitate the transport of photogenerated electrons within the nanocrystallite network. Another drawback nanocrystalline films is the existence of numerous boundaries between the nanoparticles, and therefore the diffusion of photogenerated electrons in a nanocrystalline film suffers from random walk accompanied by a series of trapping and detrapping processes (Figure 2).^[23,42] This is another pathway leading to energy loss in conventional DSCs.

2.4.2. Large Particle Light-Scatterers Resulting in a Loss of Internal Surface Area

In the double layer or mixture structure previously discussed, large TiO₂ particles (~400 nm in diameter) have been employed in the conventional DSCs for light scattering or optical reflection.

However, the use of large particles either brings about a very limited increase in the surface area of the photoelectrode film in the case of double layer structure, or unavoidably causes a decrease in the internal surface area in the case of mixture structure. This problem is particularly significant in the latter, where the large particles are embedded into the nanocrystalline film. An improvement in the structure of light scatterers, for example through using nanocrystallite aggregates as discussed in the following sections, to overcome the disadvantages of large particles serving as light scatterers is very important and could potentially boost the conversion efficiency of current DSCs.

3. DSCs with Nanocrystallite Aggregates

Nanocrystallite aggregates specifically refer to a nanostructure that comprises nanocrystallites (or nanoparticles) that assemble into a spherical agglomeration with diameters typically on the order of one micrometer. Two important features of the nanocrystallite aggregates are their sub-micrometer size comparable to the wavelengths of visible light and their porous structure arising from nanocrystallites as the building units. These features allow the nanocrystallite aggregates to serve as light scatterers in DSCs. However, unlike solid-core large particles, in the case of double layer structure the nanocrystallite aggregates may significantly increase the internal surface area of the photoelectrode film for better dye adsorption and, in the case of mixture structure, the use of nanocrystallite aggregates as light scatterers does not cause an appreciable loss in the internal surface area of the photoelectrode film.^[28,29,43] In addition to providing large surface area and light scattering, recently published literature has demonstrated more advantages of the nanocrystallite aggregates in DSC applications. For example, the compact structure inside the aggregates may provide better transport for photogenerated electrons than that in a nanocrystalline film.^[30] Photoelectrode films consisting of nanocrystallite aggregates also appear to give rise to a relatively open structure and therefore are able to facilitate the diffusion of ions in the electrolyte during solar cell operation.^[44]

3.1. Nanocrystallite Aggregates for Light Scattering

3.1.1. ZnO Aggregates

ZnO aggregates were reported in 2007 as the first use of the nanocrystallite aggregate structure for DSCs.^[28] The main ideas put forth in the research were that the aggregate structure could provide a large surface area and also generate light scattering, significantly extending the traveling distance of incident light within the photoelectrode film and thus increasing the probability of interaction between the photons and the dye molecules. The increased traveling distance contributed to enhancing the optical absorption of the photoelectrode and produced an overall efficiency of 3.5%, which was much higher than the 0.6% obtained for commercial ZnO powder. A subsequent study employed multiple dispersed aggregates (i.e., aggregates of varying diameters) to generate more effective light scattering than mono-disperse aggregates and, moreover, the pore size of

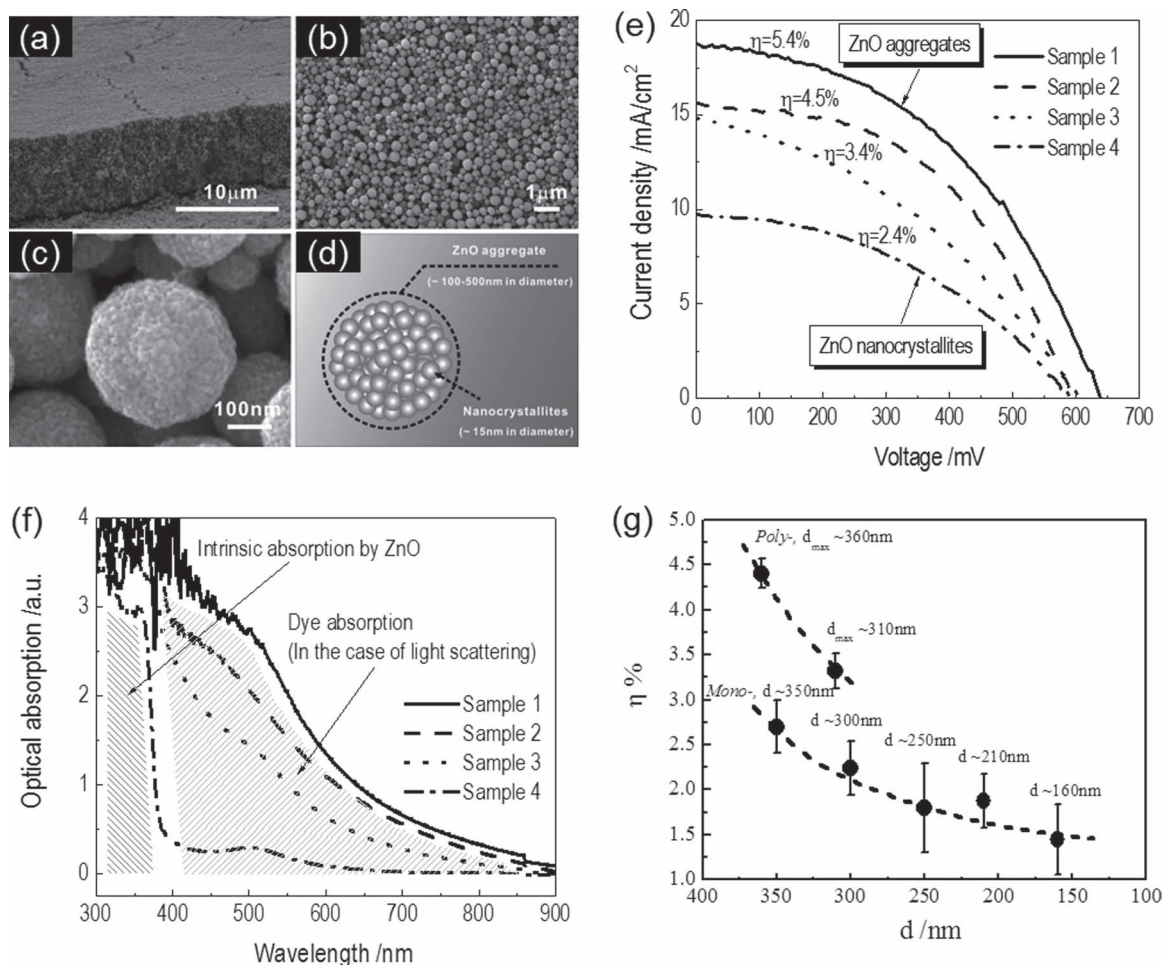


Figure 3. ZnO nanocrystallite aggregates for DSC application. (a)–(d) Morphology and structure of ZnO nanocrystallite aggregates, (e) gradually decreasing solar cell efficiency as the ZnO evolves from spherical aggregates (Sample 1) to dispersed nanocrystallites (Sample 4), (f) optical absorption spectra of ZnO Samples 1–4, and (g) dependence of overall conversion efficiency on the aggregate size and the size distribution. Reproduced with permission^[29,45] Copyright 2008, Wiley-VCH Verlag GmbH & Co. KGaA, Weinheim.

the aggregates was optimized through lowering the annealing temperature from 450 °C to 350 °C, leading to yielding efficiency as high as 5.4%, more than two times higher than the 2.4% obtained for ZnO nanoparticles.^[29] The inference that the enhancement originated from light scattering was confirmed by comparing a group of photoelectrode films that included perfectly spherical ZnO aggregates (sample 1), deconstructed ZnO aggregates that partially lost the spherical morphology (samples 2 and 3), and dispersed ZnO nanoparticles (sample 4). As expected, the result indicated a gradually decrease in the efficiency while the film structure evolved from aggregates to nanoparticles (Figure 3).

The light scattering enhancement mechanism was further supported by another study which revealed that the conversion efficiency was dependent on the size and size distribution of the aggregates. The highest efficiency was obtained from a photoelectrode film that consisted of polydisperse ZnO aggregates with an average size nearest to the wavelengths of the visible light and, as a result, generated the most intensive light scattering (Figure 3).^[45]

3.1.2. TiO₂ Coating on ZnO Aggregates

ZnO presents a similar energy band structure to that of TiO₂ and is known to be a material usable to create a variety of nanostructures. However, when used for DSCs, ZnO has typically yielded efficiencies much lower than those of TiO₂. A primary reason for the poorer performance is that ZnO is chemically unstable in the acidic dye solution containing the ruthenium complexes. This results in the formation of a Zn²⁺/dye complex on the surface of ZnO if long term sensitization is adopted.^[46] The Zn²⁺/dye complex is inactive to electron injection, which leads to low efficiency. To avoid the formation of Zn²⁺/dye complexes, one can adopt a short term sensitization (for example, 30 min), however this in turn brings about insufficient dye adsorption to the photoelectrode film. The initial motivation for coating a layer of TiO₂ onto the ZnO was to improve the stability of ZnO in the dye solution. Atomic layer deposition (ALD) was employed for this purpose since it operates under vapor conditions, allowing complete penetration of TiO₂ precursor into the photoelectrode film. Another reason

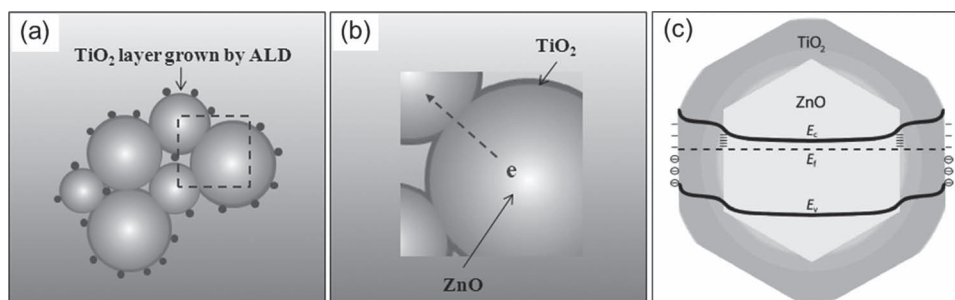


Figure 4. Fabrication of an ultrathin TiO₂ layer on ZnO aggregates through ALD. (a) and (b) Schematic drawing of TiO₂ coating on ZnO aggregates, and (c) energy level diagram of ZnO-TiO₂ core-shell structure in cross section and in equilibrium with the surrounding electrolyte. Reproduced with permission.^[47,48] [47] Copyright 2010, Wiley-VCH Verlag GmbH & Co. KGaA, Weinheim. [48] Copyright 2006, American Chemical Society.

for employing ALD was to achieve an ultrathin coating on the ZnO aggregates, preventing an appreciable decrease in the pore volume of the photoelectrode film.

The results reported in 2010 demonstrated an improvement in the solar cell efficiency, which increased from 5.2% for bare ZnO aggregates to 6.3% for TiO₂-coated ZnO aggregates.^[47] However, while the TiO₂ coating was expected to improve the surface stability of ZnO and thus achieve better dye adsorption, it was found that the coating actually generated an increase in the open-circuit voltage (V_{OC}) instead of the photocurrent density. This result is similar to what was observed in another study reported by Law et al. In that study, an ALD coating of TiO₂ thin layer on ZnO nanowires for DSC application also resulted in an increase in the V_{OC} rather than an increase in the photocurrent density.^[48] Law et al. suggested that the increase of the V_{OC} after coating with TiO₂ was due to the formation of an energy barrier on the ZnO surface that reduced the charge recombination rate and thus increased the electron concentration in the ZnO core. The increased electron concentration in the ZnO core led to a drift of the equivalent Fermi level (E_F) of the ZnO toward the bottom of the conduction band (Figure 4). The failure of the coating to enhance the photocurrent was ascribed to non-ideal crystallinity of the TiO₂ which likely gave rise to a high density of electron traps and thus offset the benefits of increased dye adsorption.

3.1.3. ZnO Aggregates Synthesized in the Presence of Lithium Ions

The surface of ZnO aggregates can be modified by including lithium ions in the synthesis of ZnO aggregates.^[49] The presence of lithium ions affects the ZnO aggregates by: 1) broadening the size distribution of the aggregates to generate more light scattering; 2) creating in an oxygen-enriched ZnO surface which gives rise to improved chemical stability of ZnO and thus suppressing the formation of Zn²⁺/dye complex that was inactive to electron injection; and 3) changing the surface chemistry of ZnO and strengthening the chemical bonding between the ZnO and the dye molecules, thus leading to more efficient electron injection from the dye molecules to the ZnO compared to pure ZnO aggregates. The DSCs with ZnO aggregates synthesized in the presence of lithium ions demonstrated conversion efficiency of 6.1%, higher than the 4.0–5.4% achieved for the pure ZnO aggregates synthesized in the absence of lithium ions (Figure 5). No lithium element is detectable in the product

of ZnO aggregates, suggesting that the lithium is neither doped into nor adsorbed onto the ZnO, but only affects the structure of the ZnO aggregates and the surface chemistry of the ZnO nanocrystallites that form the aggregates.

3.1.4. TiO₂ Aggregates Produced with an Electrospray Method

Electrospray is an electrostatic force method which can be employed to produce nanocrystallite aggregates. The mechanism of electrospray is based on an electrostatic field-induced polarization (a separation of positive and negative charges along the electric field) in individual liquid drops. The intensity of the electrostatic field applied to the liquid drop is given by^[50]

$$E = \frac{2V}{r \ln(4d/r)} \quad (1)$$

where V is the voltage applied to a needle-like nozzle where the liquid drop forms, r is the radius of the liquid drop, and d is the distance from the nozzle to the grounded electrode. When the voltage reaches a certain threshold, the liquid drop at the tip of nozzle will form a Taylor cone and emits a liquid jet through the apex of the Taylor cone. Depending on the evaporation rate, viscosity, surface tension, conductivity, and relative permittivity of the precursor solution that forms the liquid drop, the jetted liquid consisting of highly charged droplets concentrates to one-dimensional fibers or spherical structures typically having submicron dimensions.

To create nanocrystallite aggregates using the electrospray method, nanoparticles are mixed with an appropriate solvent to form a stable suspension. During the electrospray, quick evaporation of solvent from the droplets while they fly from the nozzle to the grounded electrode leads to the formation of spherical assemblies of nanoparticles, i.e., desired aggregates (Figure 6). The size of nanocrystallite aggregates produced with the electrospray method is related to factors that include the applied voltage, the solvent employed, the viscosity and surface tension of the suspension, etc. The porosity of the aggregates can be easily adjusted by, for example, adding polymer to the suspension and then removing it through a post-thermal treatment.

A good example of employing the electrospray method for the fabrication of TiO₂ nanocrystallite aggregates for DSCs was reported by Xi et al. in 2011.^[51] P25, a well-known commercial TiO₂ nanoparticles (Degussa, Germany), was dispersed into

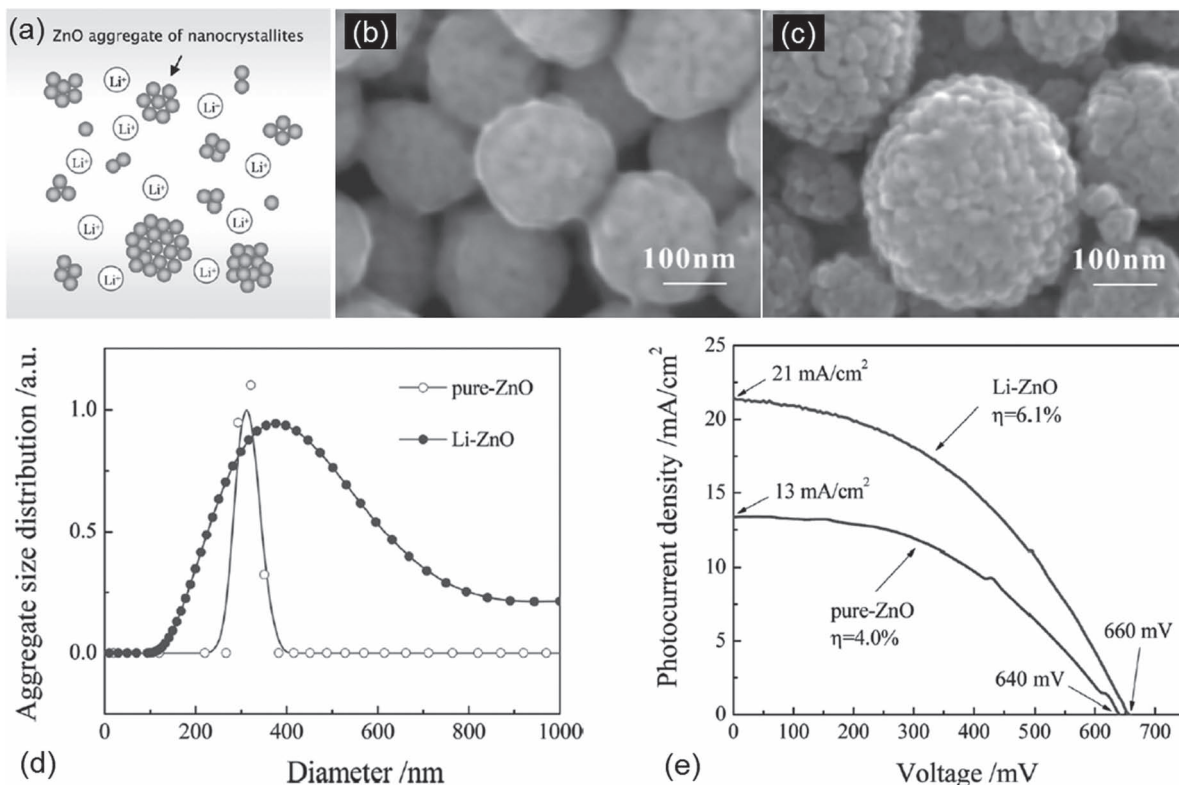


Figure 5. ZnO aggregates synthesized in the presence of lithium ions. (a) A schematic drawing of lithium ions affecting the growth of ZnO aggregates, (b) and (c) dye-sensitized ZnO aggregates synthesized in the absence (pure-ZnO) and presence (Li-ZnO) of lithium ions, respectively, implying an improved surface stability of the latter, (d) Size distribution, and (e) photovoltaic response of pure-ZnO and Li-ZnO aggregates. Reproduced with permission.^[49] Copyright 2010, American Chemical Society.

an ethanol-water (1:1, v/v) mixture solvent to form a suspension. PVP (polyvinylpyrrolidone, $MW \approx 1.3 \times 10^6$) was added to the suspension to increase the viscosity and, as thus, adjust the porosity of the aggregates. The as-prepared nanocrystallite aggregates were studied for their DSC performance. Note that the PVP additive was removed during the photoelectrode film

was applied a thermal treatment at 450 °C. It was reported that a 5.9% efficiency was obtained using the aggregates. Such an efficiency was significantly higher than the 4.8% obtained for dispersed P25 nanoparticles. A comparison of the dye adsorption between the photoelectrode film consisting of nanocrystallite aggregates and that made of dispersed nanoparticles revealed

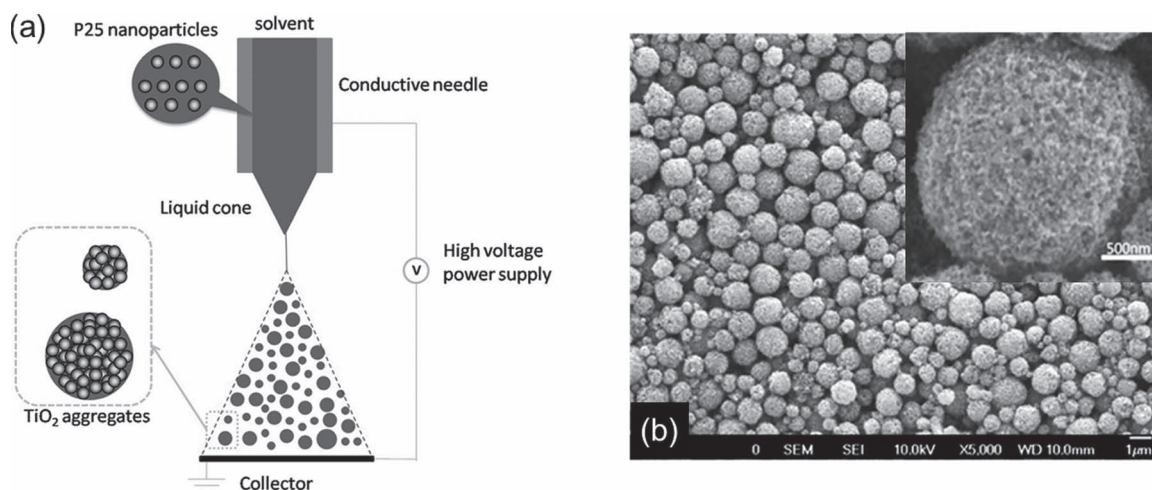


Figure 6. Electrospray method for the fabrication of TiO₂ nanocrystallite aggregates. (a) Schematic diagram showing set-up for electro-spray fabrication of TiO₂ nanocrystallite aggregates, and (b) SEM images of TiO₂ nanocrystallite aggregates produced with an electro-spray method. Reproduced with permission.^[51] Copyright 2011, American Scientific Publishers.

that the former achieved less dye adsorption than the latter. This was explained by the existence of large voids in the aggregate film and therefore a smaller internal surface area of the aggregate film compared to the nanoparticle film. However, the fact that a higher efficiency was received for the aggregate film than the nanoparticle film strongly suggested that the light scattering played an important role in enhancing the optical absorption as well as the solar-to-electricity conversion of the cell.

3.1.5. Mesoporous TiO₂ Beads

Single Layer Structure: Mesoporous TiO₂ beads, which were reported by Chen et al. in 2009, presented a structure similar to the ZnO aggregates, i.e., spherical assemblies constructed with nano-sized crystallites.^[52] The mesoporous TiO₂ beads were created through a two-step method, which involved the first step synthesis of submicron-sized solid TiO₂ spheres and the second step hydrothermal growth that etched the TiO₂ spheres to be of porous structure and transformed the TiO₂ from the amorphous phase to the crystalline one.^[53] A characterization of the DSC performance of the mesoporous TiO₂ beads demonstrated an efficiency of 7.20%, which was higher than the 5.66% obtained for P25 nanoparticles. This phenomenon was explained by a light scattering mechanism evidenced by measured diffuse reflectance spectra, on which P25 nanoparticles serving as reference only showed a diffuse reflection capacity in the wavelength range of 400 nm to 450 nm, which quickly dropped as the wavelength increased from 450 nm to 800 nm; the mesoporous beads, however, displayed a high diffuse reflection capacity

in the entire visible and near-infrared regions from 400 nm to 800 nm (Figure 7).

Double Layer and Mixture Structures: In addition to using mesoporous beads to form single layer structured photoelectrode films, there have been several attempts to employ the mesoporous TiO₂ beads in double layer or mixture structured DSCs as light scatterers.^[54,55] Recent work reported by Huang et al. compared the mesoporous TiO₂ beads and the 400-nm large particles in term of their light scattering effect when used in double layer structured DSCs.^[55] The photoelectrode film with mesoporous TiO₂ beads as the light scattering layer demonstrated 8.84% efficiency, higher than that of the 7.87% with 400-nm large particles. This implied that the porous structured aggregates might achieve additional dye adsorption and thus contributed to the optical absorption as well as the solar cell efficiency.

The use of nanocrystallite aggregates as light scatterers in a mixture structure has also demonstrated 30%-40% increase in the conversion efficiency when compared with the photoelectrode film that consists of nanoparticles alone.^[56,57] However, the existing empirical data in the literature cannot clarify the extent to which the nanocrystallite aggregates perform better than the solid-core large particles while mixed into a nanocrystalline film.

3.2. Nanocrystallite Aggregates with Open Structures Facilitating Ion Diffusion

In addition to the light scattering mechanism, the open structure of the photoelectrode film consisting of nanocrystallite

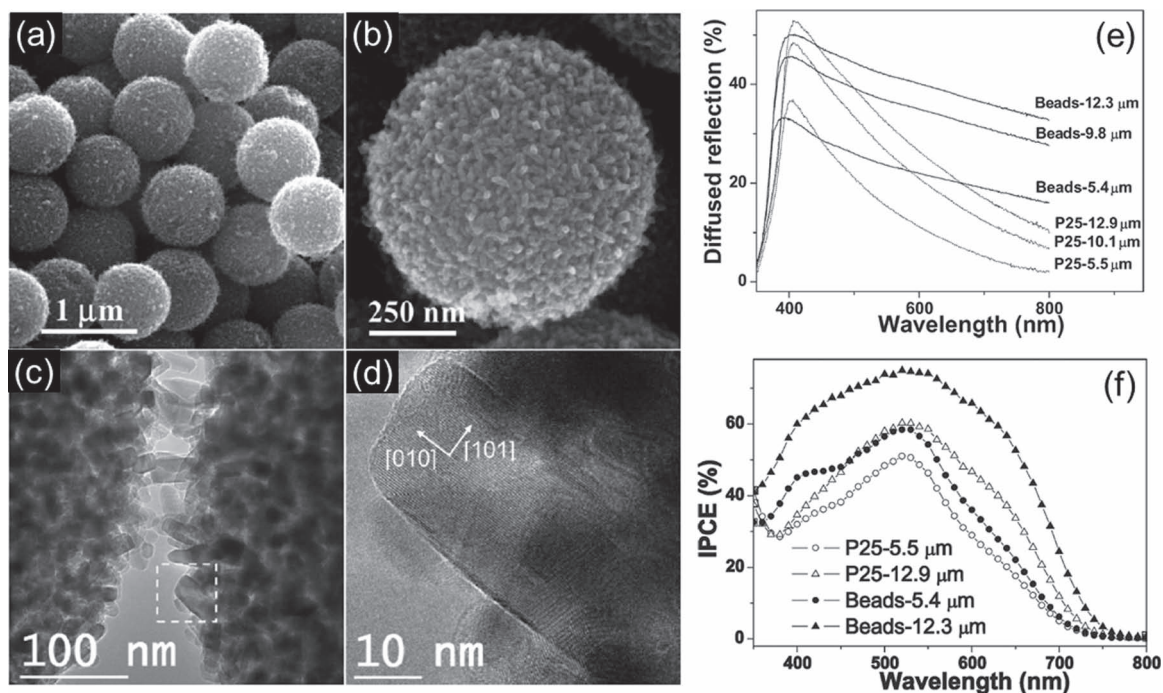


Figure 7. Mesoporous TiO₂ beads for DSC application. (a)–(d) Morphology and structure of mesoporous TiO₂ beads produced with a two-step method, (e) diffuse reflectance spectra of P25 nanoparticle films and mesoporous bead films in different thickness, and (f) incident photo to current conversion efficiency (IPCE) curves of P25 nanoparticle films and mesoporous bead films. Reproduced with permission.^[52,53] [52] Copyright 2009, Wiley-VCH Verlag GmbH & Co. KGaA, Weinheim. [53] Copyright 2010, American Chemical Society.

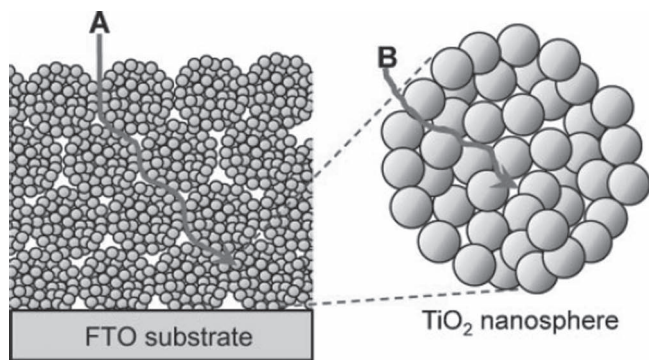


Figure 8. Open structure of photoelectrode film comprised of nanoporous TiO₂ spheres for facilitating the diffusion of electrolyte through external pores (A) and internal pores (B).^[44] Copyright 2010, Wiley-VCH Verlag GmbH & Co. KGaA, Weinheim.

aggregates has been identified as another factor that contributes to improved DSC efficiency. The so-called “open structure” arises from the large voids that exist among the aggregates. It is suggested that these large voids serve as a “highway” that allows fast diffusion of I₃⁻ ions (in electrolyte) within the photoelectrode film (Figure 8). A measurement of the ion diffusion constants revealed that the ion diffusion constant in the photoelectrode with TiO₂ aggregates is $6.7 \times 10^{-6} \text{ cm}^2 \text{ s}^{-1}$, larger than that of $4.1 \times 10^{-6} \text{ cm}^2 \text{ s}^{-1}$ in the photoelectrode with dispersed nanoparticles.^[44] As a result, the DSCs with aggregate films achieved 8.44% efficiency, higher than the 7.3% for the nanoparticle films.

3.3. Tightly Interconnected Nanocrystallites within the Aggregates Enhancing Electron Transport

Besides the hypotheses of light scattering enhancing optical absorption and the open structure of the aggregate film facilitating the electrolyte diffusion, Sauvage et al. in 2010 suggested that the nanocrystallites within the aggregates were tightly interconnected and that such a compact structure might benefit the DSCs by facilitating electron transport.^[30] Experiments showed that the photoelectrode film constructed with mesoporous TiO₂

beads presented a longer electron diffusion length than the film comprised of dispersed P25 nanoparticles (Figure 9). This implied that the compact interconnection of nanocrystallites within individual aggregates could achieve efficient electron transport and reduce charge recombination in DSCs. This led to 9.1% efficiency for the cell with mesoporous TiO₂ beads compared with 7.1% for P25 nanoparticles.

Recently reported work by Yan et al. measured the values of the electron diffusion coefficient (D_n) for the photoelectrode film with mesoporous TiO₂ microspheres. The values obtained were five times higher than those for the photoelectrode film with P25 nanoparticles (Figure 9).^[54] Since the difference in the electron lifetime (τ_n) between the films, however, was small, following the formula $L_n = (D_n \tau_n)^{1/2}$, the electron diffusion length (L_n) in the mesoporous TiO₂ microsphere film was estimated to be approximately five-times longer than in a nanoparticle film.

4. Summary

4.1. Multiple Functions of the Nanocrystallite Aggregates

Nanocrystallite aggregates have been intensively studied over recent years for application to DSCs. The overall results of these studies have demonstrated that the photoelectrode films formed from nanocrystallite aggregates can generate efficiencies higher than (in the case of ZnO) or comparable to (in the case of TiO₂) those made with dispersed nanoparticles. When used as light scatterers, the nanocrystallite aggregates can also perform better than the 400-nm solid-core particles commonly employed in DSCs. Multiple mechanisms have been proposed to explain the improved DSC performance of the nanocrystallite aggregates. Most studies have emphasized the large surface area of the aggregates. The internal surface area of photoelectrode films with the nanocrystallite aggregates is comparable to or even larger than that of those with nanoparticles. This is the *primary merit* of the nanocrystallite aggregates, allowing the aggregates to be appropriate for application to DSCs for achieving sufficient dye adsorption while serving as photoelectrode film. *Another merit* that has also been stressed is the capability of the aggregates for light scattering, which results

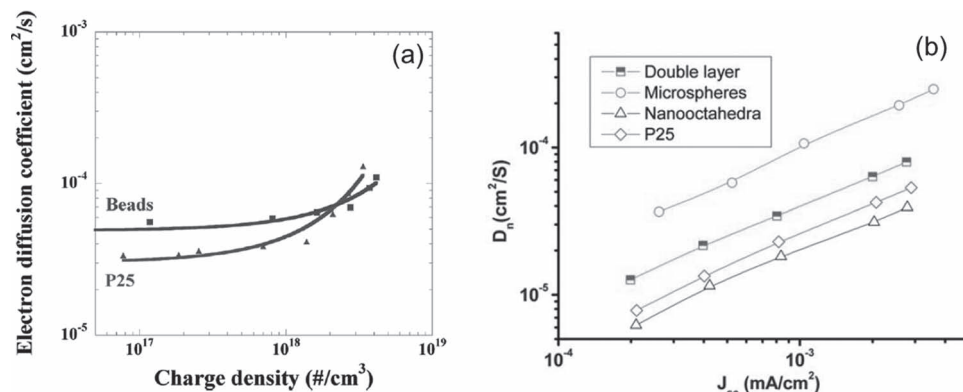


Figure 9. Comparisons of electron diffusion in photoelectrode films constructed with mesoporous TiO₂ beads (or microspheres) or P25 nanoparticles. (a) and (b) The dependence of electron diffusion coefficients on charge density and short-circuit current, respectively.^[30,54] [30] Copyright 2010, American Chemical Society. [54] Copyright 2011, The Royal Society of Chemistry.

from the sub-micrometer size of the aggregates being comparable to the wavelengths of visible light. *The third merit* of the nanocrystallite aggregates is the compact interconnection of the nanocrystallites within individual aggregates. The compact interconnection enables highly efficient electron transport and results in an electron diffusion length in the photoelectrode film comprising aggregates longer than that in a film made of dispersed nanoparticles. Finally, *one more merit* that has also been suggested in literature is the relatively open structure of the nanocrystallite aggregate photoelectrode films, which creates paths for quick diffusion of the electrolyte (I_3^- ions) during solar cell operation.

4.2. The Formation of Oxide Nanocrystallite Aggregates

The formation of oxide nanocrystallite aggregates very much depends on the materials themselves especially in terms of their crystalline properties and the surface chemistry of the nanocrystallites. While the aggregates are used for DSCs, not only the geometric shape but also the size and porosity of the aggregates and the facets of the nanocrystallites forming the aggregates should be carefully considered in matching the requirements for dye adsorption, electrolyte diffusion, electron transport, and the generation of effective light scattering. There are many approaches that can be adopted to create the nanocrystallite aggregate structure (or spherical mesoporous structure), such as self-assembly, electrospray/ultrasonic spray, two-step etching, and template method.

4.2.1. Self-Assembly

The formation of ZnO aggregates introduced above is a typical process of *self-assembly* of nanocrystallites occurring during the hydrolysis of zinc salt in a polyol medium at elevated temperature (160 °C).^[29,58] A model developed by Tay et al. suggests that an initial hydrolysis of zinc salt generates high concentrated ZnO nanocrystallites in the solution. These nanocrystallites possess Zn-exposed (0001) plane and O-exposed (000 $\bar{1}$) plane, which are positively charged and negatively charged, respectively. Therefore, individual nanocrystallites can be regarded as polar entities and, due to the existence of strong attractive forces, they trend to agglomerate and form spherical arrangement, which is a configuration much more stable than the individual nanocrystallites having polar surfaces, so as to minimize the surface energy.^[59] Self-assembly to form aggregates can be also achieved by surface modification of oxide nanocrystallites using polymer additives^[60] or inorganic salts such as ammonium citrate,^[61] which attach on the surface of oxide nanocrystallites to facilitate the connection of the nanocrystallites, leading to the formation of spherical aggregates.

Another very important mechanism that may also result in the formation of nanocrystallite aggregate structure through self-assembly is the *Ostwald Ripening*, which is a phenomenon observed in liquid sols describing a dissolution of small particles and then re-deposition to form large particles; the latter is more energetically favored than the former.^[62] There are quite a few examples regarding the fabrication of spherical mesoporous structure of TiO₂ under hydrothermal conditions based on the Ostwald Ripening mechanism reported recently.^[63,64]

One of advantages of the self-assembly method is its high-efficiency mass production. However, a drawback of this method is its difficulty in controlling the facets of the nanocrystallites to maximally match the requirement for dye adsorption. This point is critically important especially in the case of TiO₂. As mentioned above, only anatase TiO₂ with exposed (101) facet may achieve the most ideal dye adsorption and meanwhile the most efficient electron injection.^[40]

4.2.2. Electrospray and Ultrasonic Spray

Electrospray and ultrasonic spray are a kind of mechanical approach for the fabrication of nanocrystallite aggregates, in which liquid drops containing nanocrystallites (or nanoparticles) are generated firstly through an electrostatic field^[51] or ultrasonic atomization principle.^[65] The liquid drops lose the solvent during their consequent flight to the collector, leading to the formation of spherical aggregates of nanoparticles. The most outstanding merit of the spray method is that it may start with nanocrystallites which, importantly, can be produced in advance. This enables to choose the nanocrystallites with suitable crystal phase and desired facets for the formation of aggregates. However, the spray method suffers from the drawbacks of low production efficiency and difficulty in receiving small-sized aggregates (<1 μm).

4.2.3. Two-Step Synthetic Approach

Two-step synthesis is a method based on an etching of submicron-sized solid spheres that are produced in the first step. The as-produced solid spheres then undergo a treatment in a designed solution that may etch the spheres and convert them to a mesoporous structure.^[66] This method has been extensively reported recently for the preparation of TiO₂ mesoporous spheres for application to DSCs, demonstrating quite high efficiencies.^[44,52] Speaking strictly, the mesoporous spheres fabricated with this approach is not exactly the same as the structure of nanocrystallite aggregates produced with a self-assembly or spray method discussed above. However, while used for DSCs, both the mesoporous spheres and the nanocrystallite aggregates present bifunction of providing large internal surface area for dye adsorption and meanwhile generating effective light scattering that may enhance optical absorption.

The disadvantage of the two-step synthetic approach is that the nanocrystallites are created with an etching process and they therefore can not offer ideal crystallinity and desired facets for the achievement of optimal dye adsorption and electron injection.

4.2.4. Template Method

Template method is a way that restricts the nanocrystallites in spherical template which plays a role of space confinement and leads to the formation of nanocrystallite aggregates after the template is removed. Carbon spheres are a type of typical template that has been employed for the preparation of nanocrystallite aggregates of metal oxides including TiO₂.^[67] To use water-in-oil emulsion system is another potential way that can produce the nanocrystallite aggregates. In this method,

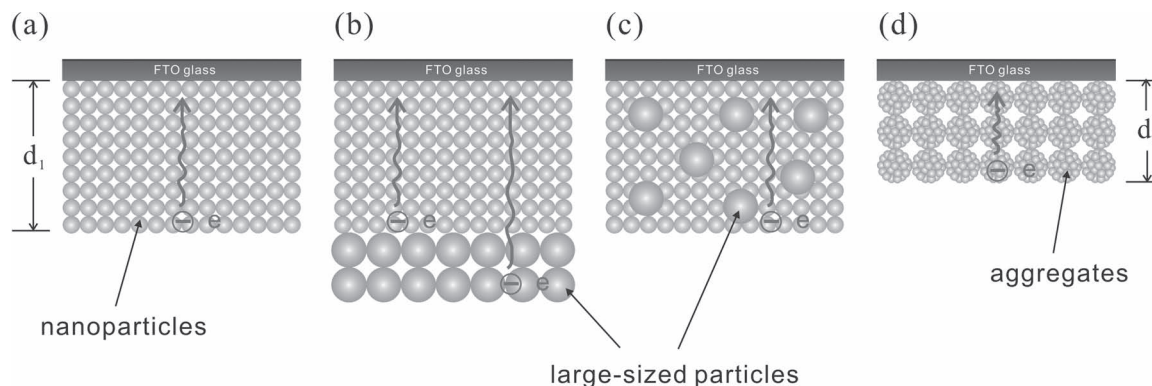


Figure 10. Schematic drawing showing different electron transport distances in (a) nanocrystalline film, (b) double structure, (c) mixture structure including ~400-nm large particles for light scattering, and (d) single layer structured photoelectrode film with nanocrystalline aggregates. The transport distance (d_2) in nanocrystallite aggregate film is smaller than that (d_1) in other structured photoelectrode films.

individual water droplets dispersed in the emulsion are kind of micro-reactors which can serve as a *soft-template* for the growth of nanocrystallites and the formation of aggregate structure.

5. Perspectives

5.1. Reduction of the Photoelectrode film Thickness to Reduce the Charge Recombination Rate in DSCs

Nanocrystallite aggregates appear to generate effective light scattering and thus enhance the light harvesting efficiency of photoelectrode film. The improved light harvesting efficiency therefore makes it possible to create thinner photoelectrode films than those made of nanoparticles without decreasing the optical absorption of the photoelectrode. The benefit of reducing the photoelectrode film thickness is to shorten the transport distance of the photogenerated electrons (**Figure 10**). The reduced transport distance should in turn lower the charge recombination rate in the solar cell, therefore resulting in an increase in both the open-circuit voltage and photocurrent density. Thus the photoelectrode film composed of nanocrystallite aggregates with thickness less than that of nanocrystalline film in the conventional DSCs may possibly lead to a breakthrough in the efficiency of DSCs. The improved electron transport within the aggregates due to a tight interconnection of the nanocrystallites would also contribute to diminishing the charge recombination rate and boost the efficiency of the DSCs even further.

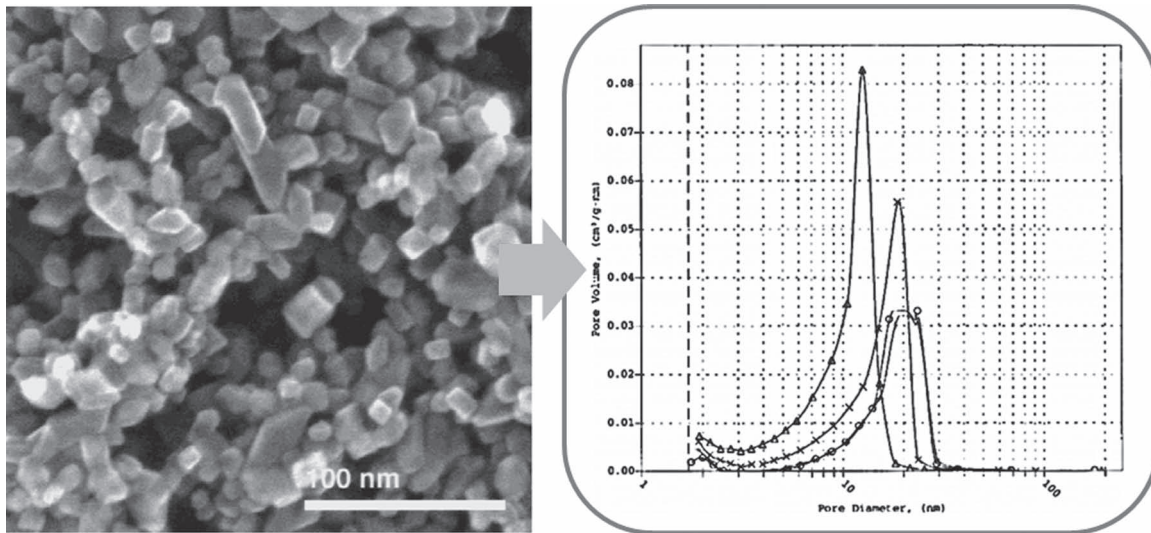
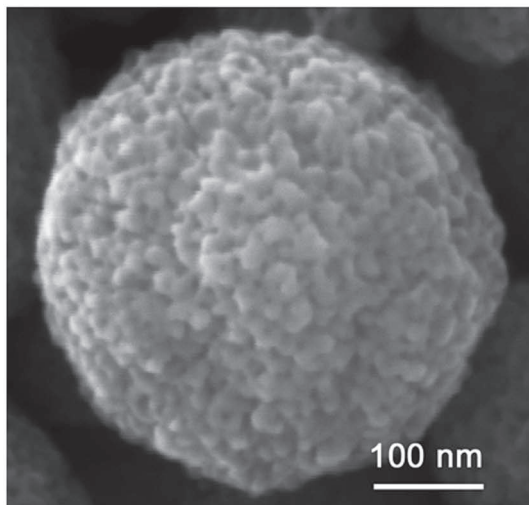
5.2. Optimization of the Porosity of Aggregates and the Facets of Nanocrystallites Forming the Aggregates

The advantages of the nanocrystallite aggregates films discussed in this paper have included large surface areas, light harvesting-enhanced optical absorption, improved electron transport, and an open structure facilitating electrolyte diffusion. However, in order to reach the full performance potential of the nanocrystallite aggregates in DSCs, it is likely that the porosity (especially contributed by relatively small pores) of the aggregates and

the facets of the nanocrystallites that form the aggregates still require significant efforts for optimization.

The pore sizes of the aggregates reported in the existing literature are typically on the order of several nanometers.^[29,43] These pore sizes are much smaller than those in conventional photoelectrode films made of nanocrystallites with polymer binders, where the pores are about 10 nm or larger (**Figure 11**).^[40] A smaller porosity resulting in a more compact structure is preferred for efficient electron transport. However, if the pores are too small, they might not permit complete penetration of the dye solution into the aggregates or allow quick diffusion of electrolyte within the photoelectrode film. These factors could explain why current TiO₂ nanocrystallite aggregate DSCs have not achieved power conversion efficiencies (PCEs) exceeding those of conventional nanocrystallite DSCs. Optimization of the porosity and pore size of the aggregates could bring a significant enhancement in the PCE of DSCs by balancing the conflicting requirements of dye adsorption, electrolyte diffusion, and electron transport in aggregate-based DSCs.

While the porosity of the photoelectrode film directly affects the internal surface area of the film and therefore the dye adsorption amount, the facets of TiO₂ nanocrystallites may also play an important role in affecting the dye adsorption. Previous work has suggested that anatase TiO₂ with exposed (101) facet may achieve the most successful dye adsorption. Fortuitously, nanoparticles produced by hydrothermally hydrolyzing titanium alkoxide in an acidic aqueous solution predominantly present (101) facet.^[40] However, the exposed nanocrystallite facet has not been addressed in most of the reported methods for the synthesis of TiO₂ nanocrystallite aggregates, especially the two-step method where the aggregates are created through etching of solid spheres. This suggests that development of fabrication methods towards creating TiO₂ aggregates comprised of nanocrystallites with principally exposed (101) facet would no doubt bring about a significant improvement in dye adsorption and, as such, further boost the efficiency of DSCs with photoelectrode film consisting of TiO₂ nanocrystallite aggregates. It is worthy of pointing out that the electrospray mentioned above,^[51,57] which starts with a nanoparticle dispersed suspension, is such a method that may preserve the facets of the nanoparticles when

(a) TiO₂ nanocrystalline film

(b) ZnO aggregates

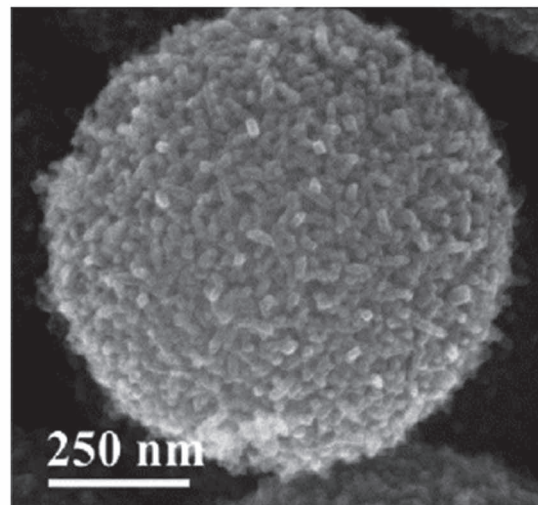
(c) TiO₂ Aggregates

Figure 11. SEM images of TiO₂ nanocrystalline film with pore size distribution (a),^[40] ZnO aggregates (b),^[29] and TiO₂ aggregates (c)^[53] presenting apparent difference of these nanostructures in the sizes of pores and nanocrystallites. [29] Copyright 2008, Wiley-VCH Verlag GmbH & Co. KGaA, Weinheim. [40] Copyright 1997, The American Ceramic Society. [53] Copyright 2010, American Chemical Society.

they are assembled into aggregates. However, this method suffers from a low efficiency in materials synthesis.

5.3. Optimal Double Layer Structure to Maximize Light Harvesting

Nanocrystallite aggregates are such a material that can form photoelectrode film achieving high efficiency in a single layer in view of the advantages mentioned above in the aspects of dye adsorption, light scattering, electron transport, and electrolyte diffusion.^[30] However, a photoelectrode film with single layer is not thought to be an optimal structure for light harvesting for the reason that there exists reflection to the incident light by the

nanocrystallite aggregates at the interface between the FTO and aggregate films (Figure 10d). To solve this problem, a double layer structure is proposed to absorb the light reflected by the aggregates by adding a layer of nanocrystalline film in front of the aggregate layer (Figure 12). Note that the proposed double layer structure is different from that in conventional double-layer DSCs, which typically includes a 12 μm thick nanocrystalline film serving as an active layer covered by a 4 μm thick light scattering layer comprised of ~400 nm particles (i.e., a “12 μm + 4 μm” mode) (Figure 1a).^[68] In the proposed photoelectrode based on nanocrystallite aggregates, the double layer structure would be a thin nanocrystalline film covered by a thick nanocrystallite aggregate film. In this structure, the active layer is the nanocrystallite aggregate film instead of the nanocrystalline

incident light

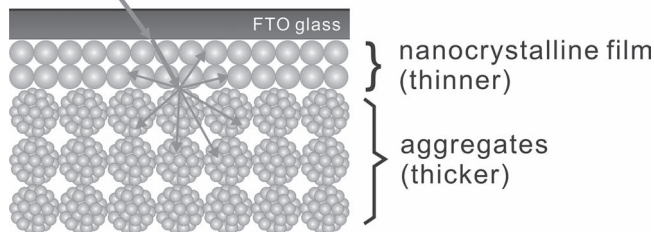


Figure 12. Proposed double layer structured photoelectrode with an optimization consideration for optical absorption enhancement by avoiding the loss of incident light from being directly reflected by the aggregate layer.

film, as such, to maximize the benefits of nanocrystallite aggregates to DSCs in terms of light scattering, electron transport, and electrolyte diffusion. Support for the idea of employing a double layer structure in which the nanocrystallite aggregate film serves as the active layer can be seen to some extent in recent work performed by Huang et al.^[55] and Yu et al.^[69] In these studies, the highest efficiencies were achieved with double layer structured photoelectrodes having a “6.3 μm + 11 μm ” or “9 μm + 11 μm ” mode. These two modes, with the bottom layer comprised of TiO_2 nanoparticles thinner than the top layer consisting of nanocrystallite aggregates, is opposite to the conventional double structure with a “12 μm + 4 μm ” mode.

Compared with the single layer structured photoelectrode made of nanocrystallite aggregates as discussed in Section 5.1, in the proposed double layer structure, the insertion of a thin layer of nanocrystalline film may somewhat increase the charge recombination of the cell due to an increased thickness of the photoelectrode film. However, it is anticipated that the adverse effect of the charge recombination on the photocurrent could be compensated by the enhanced optical absorption in view of the nanocrystalline film absorbing the light reflected by the aggregate layer.

6. Conclusions

It can be summarized that the superiority of nanocrystallite aggregates for DSC applications arises from: 1) their ability to generate light scattering while avoiding the loss of internal surface area that occurs with solid-core large particle light scatterers; 2) the improvement of electron transport resulting from a tight interconnection of nanocrystallites within the aggregates; and 3) the facilitation of electrolyte diffusion through the relatively open structure of the photoelectrode film created by the aggregates. ZnO aggregates have demonstrated a more than twofold increase in overall DSC conversion efficiency compared with the dispersed ZnO nanoparticles. The TiO_2 aggregates in a single layer have the capability of achieving very high efficiencies comparable to the record ~10–11% efficiencies achieved by TiO_2 nanoparticles with double layer structure. Nanocrystallite aggregates thus considered to be a promising material that may potentially lead to breakthroughs in improving the conversion

efficiency of DSCs by further optimization in terms of the structure of photoelectrode film, the porosity of the aggregates, and the facets of the nanocrystallites that form the aggregates.

Acknowledgements

This work related to the ZnO aggregates, ALD surface modification, electrospray fabrication of TiO_2 aggregates, and the characterization of solar cell performance is supported by the U.S. Department of Energy, Office of Basic Energy Sciences, Division of Materials Sciences, under Award No. DE-FG02-07ER46467 (Q.F.Z.). This work is also supported in part by the National Science Foundation (DMR 1035196), the Air Force Office of Scientific Research (AFOSR-MURI, FA9550-06-1-0326), the University of Washington TGIF grant, the Royalty Research Fund (RRF) from the Office of Research at University of Washington, the Washington Research Foundation, and the Intel Corporation.

Received: June 25, 2011

Revised: September 21, 2011

- [1] M. Grätzel, *Nature* **2001**, 414, 338.
- [2] A. Hagfeldt, G. Boschloo, L. Sun, L. Kloo, H. Pettersson, *Chem. Rev.* **2010**, 110, 6595.
- [3] M. Grätzel, *J. Photochem. Photobiol. C: Photochem. Rev.* **2003**, 4, 145.
- [4] A. Hagfeldt, M. Grätzel, *Acc. Chem. Res.* **2000**, 33, 269.
- [5] M. Grätzel, *Inorg. Chem.* **2005**, 44, 6841.
- [6] Q. F. Zhang, G. Z. Cao, *Nano Today* **2011**, 6, 91.
- [7] Q. F. Zhang, C. S. Dandeneau, X. Y. Zhou, G. Z. Cao, *Adv. Mater.* **2009**, 21, 4087.
- [8] A. B. F. Martinson, T. W. Hamann, M. J. Pellin, J. T. Hupp, *Chem. Eur. J.* **2008**, 14, 4458.
- [9] B. Oregan, M. Grätzel, *Nature* **1991**, 353, 737.
- [10] Y. Chiba, A. Islam, Y. Watanabe, R. Komiya, N. Koide, L. Y. Han, *Japn. J. Appl. Phys., Part 2* **2006**, 45, L638.
- [11] M. K. Nazeeruddin, F. De Angelis, S. Fantacci, A. Selloni, G. Viscardi, P. Liska, S. Ito, T. Bessho, M. Grätzel, *J. Am. Chem. Soc.* **2005**, 127, 16835.
- [12] M. K. Nazeeruddin, A. Kay, I. Rodicio, R. Humphrybaker, E. Muller, P. Liska, N. Vlachopoulos, M. Grätzel, *J. Am. Chem. Soc.* **1993**, 115, 6382.
- [13] M. K. Nazeeruddin, S. M. Zakeeruddin, R. Humphry-Baker, M. Jirousek, P. Liska, N. Vlachopoulos, V. Shklover, C. H. Fischer, M. Grätzel, *Inorg. Chem.* **1999**, 38, 6298.
- [14] M. K. Nazeeruddin, P. Pechy, T. Renouard, S. M. Zakeeruddin, R. Humphry-Baker, P. Comte, P. Liska, L. Cevey, E. Costa, V. Shklover, L. Spiccia, G. B. Deacon, M. Grätzel, *J. Am. Chem. Soc.* **2001**, 123, 1613.
- [15] P. Wang, C. Klein, R. Humphry-Baker, S. M. Zakeeruddin, M. Grätzel, *J. Am. Chem. Soc.* **2005**, 127, 808.
- [16] D. B. Kuang, S. Ito, B. Wenger, C. Klein, J. E. Moser, R. Humphry-Baker, S. M. Zakeeruddin, M. Grätzel, *J. Am. Chem. Soc.* **2006**, 128, 4146.
- [17] F. Gao, Y. Wang, D. Shi, J. Zhang, M. K. Wang, X. Y. Jing, R. Humphry-Baker, P. Wang, S. M. Zakeeruddin, M. Grätzel, *J. Am. Chem. Soc.* **2008**, 130, 10720.
- [18] C. Klein, M. K. Nazeeruddin, P. Liska, D. Di Censo, N. Hirata, E. Palomares, J. Durrant, M. Grätzel, *Inorg. Chem.* **2005**, 44, 178.
- [19] F. T. Kong, S. Y. Dai, K. J. Wang, *Adv. OptoElectron.* **2007**, 2007, 75384.
- [20] M. Grätzel, *Progr. Photovoltaics* **2000**, 8, 171.
- [21] M. Grätzel, *J. Photochem. Photobiol. A: Chemistry* **2004**, 164, 3.

- [22] H. J. Snaith, *Adv. Funct. Mater.* **2010**, *20*, 13.
- [23] J. Nelson, R. E. Chandler, *Coord. Chem. Rev.* **2004**, *248*, 1181.
- [24] M. Law, L. E. Greene, J. C. Johnson, R. Saykally, P. Yang, *Nat. Mater.* **2005**, *4*, 455.
- [25] K. Shankar, G. K. Mor, H. E. Prakasam, S. Yoriya, M. Paulose, O. K. Varghese, C. A. Grimes, *Nanotechnology* **2007**, *18*, 065707.
- [26] J. R. Jennings, F. Li, Q. Wang, *J. Phys. Chem. C* **2010**, *114*, 14665.
- [27] Q. F. Zhang, G. Z. Cao, *J. Mater. Chem.* **2011**, *21*, 6769.
- [28] T. P. Chou, Q. F. Zhang, G. E. Fryxell, G. Z. Cao, *Adv. Mater.* **2007**, *19*, 2588.
- [29] Q. F. Zhang, T. R. Chou, B. Russo, S. A. Jenekhe, G. Z. Cao, *Angew. Chem. Int. Ed.* **2008**, *47*, 2402.
- [30] F. Sauvage, D. H. Chen, P. Comte, F. Z. Huang, L. P. Heiniger, Y. B. Cheng, R. A. Caruso, M. Graetzel, *ACS Nano* **2010**, *4*, 4420.
- [31] N. Sekar, V. Y. Gehlot, *Resonance* **2010**, *15*, 819.
- [32] M. Ryan, *Platinum Met. Rev.* **2009**, *53*, 216.
- [33] N. Robertson, *Angew. Chem. Int. Ed.* **2006**, *45*, 2338.
- [34] A. S. Polo, M. K. Itokazu, N. Y. Murakami Iha, *Coord. Chem. Rev.* **2004**, *248*, 1343.
- [35] S. Ito, M. K. Nazeeruddin, S. M. Zakeeruddin, P. Pechy, P. Comte, M. Grätzel, T. Mizuno, A. Tanaka, T. Koyanagi, *Int. J. Photoenergy* **2009**, *2009*, 517609.
- [36] M. Grätzel, *Chem. Lett.* **2005**, *34*, 8.
- [37] S. Ito, T. N. Murakami, P. Comte, P. Liska, C. Grätzel, M. K. Nazeeruddin, M. Grätzel, *Thin Solid Films* **2008**, *516*, 4613.
- [38] J. Kroon, N. Bakker, H. Smit, P. Liska, K. Thampi, P. Wang, S. Zakeeruddin, M. Grätzel, A. Hinsch, S. Hore, *Progr. Photovoltaics* **2007**, *15*, 1.
- [39] J. Ferber, J. Luther, *Sol. Energy Mater. Sol. Cells* **1998**, *54*, 265.
- [40] C. J. Barbé, F. Arendse, P. Comte, M. Jirousek, F. Lenzmann, V. Shklover, M. Grätzel, *J. Am. Ceram. Soc.* **1997**, *80*, 3157.
- [41] D. Cahen, G. Hodes, M. Grätzel, J. F. Guillemoles, I. Riess, *J. Phys. Chem. B* **2000**, *104*, 2053.
- [42] J. Van de Lagemaat, N. G. Park, A. Frank, *J. Phys. Chem. B* **2000**, *104*, 2044.
- [43] Q. F. Zhang, C. S. Dandeneau, K. Park, D. W. Liu, X. Y. Zhou, Y. H. Jeong, G. Z. Cao, *J. Nanophotonics* **2010**, *4*.
- [44] Y. J. Kim, M. H. Lee, H. J. Kim, G. Lim, Y. S. Choi, N. G. Park, K. Kim, W. I. Lee, *Adv. Mater.* **2009**, *21*, 3668.
- [45] Q. F. Zhang, T. P. Chou, B. Russo, S. A. Jenekhe, G. Cao, *Adv. Funct. Mater.* **2008**, *18*, 1654.
- [46] T. P. Chou, Q. F. Zhang, G. Z. Cao, *J. Phys. Chem. C* **2007**, *111*, 18804.
- [47] K. Park, Q. F. Zhang, B. B. Garcia, X. Y. Zhou, Y. H. Jeong, G. Z. Cao, *Adv. Mater.* **2010**, *22*, 2329.
- [48] M. Law, L. E. Greene, A. Radenovic, T. Kuykendall, J. Liphardt, P. Yang, *J. Phys. Chem. B* **2006**, *110*, 22652.
- [49] Q. F. Zhang, C. S. Dandeneau, S. Candelaria, D. W. Liu, B. B. Garcia, X. Y. Zhou, Y. H. Jeong, G. Z. Cao, *Chem. Mater.* **2010**, *22*, 2427.
- [50] L. Loeb, A. Kip, G. Hudson, W. Bennett, *Phys. Rev.* **1941**, *60*, 714.
- [51] J. T. Xi, Q. F. Zhang, S. H. Xie, S. Yodyingyong, K. Park, Y. M. Sun, J. Y. Li, G. Z. Cao, *Nanosci. Nanotechnol. Lett.* **2011**, In press, DOI: 10.1166/nnl.2011.1223.
- [52] D. H. Chen, F. Z. Huang, Y. B. Cheng, R. A. Caruso, *Adv. Mater.* **2009**, *21*, 2206.
- [53] D. H. Chen, L. Cao, F. Z. Huang, P. Imperia, Y. B. Cheng, R. A. Caruso, *J. Am. Chem. Soc.* **2010**, *132*, 4438.
- [54] K. Yan, Y. Qiu, W. Chen, M. Zhang, S. Yang, *Energy Environ. Sci.* **2011**, *4*, 2168.
- [55] F. Z. Huang, D. H. Chen, X. L. Zhang, R. A. Caruso, Y. B. Cheng, *Adv. Funct. Mater.* **2010**, *20*, 1301.
- [56] S. H. Jang, Y. J. Kim, H. J. Kim, W. In Lee, *Electrochem. Commun.* **2010**, *12*, 1283.
- [57] J. T. Xi, Q. F. Zhang, K. Park, Y. M. Sun, G. Z. Cao, *Electrochim. Acta* **2011**, *56*, 1960.
- [58] D. Jezequel, J. Guenot, N. Jouini, F. Fievet, *J. Mater. Res.* **1995**, *10*, 77.
- [59] Y. Y. Tay, S. Li, F. Boey, Y. H. Cheng, M. H. Liang, *Phys. B* **2007**, *394*, 372.
- [60] S. Eiden-Assmann, J. Widoniak, G. Maret, *J. Dispersion Sci. Technol.* **2004**, *25*, 535.
- [61] Y. X. Zhang, G. H. Li, Y. C. Wu, Y. Y. Luo, L. D. Zhang, *J. Phys. Chem. B* **2005**, *109*, 5478.
- [62] A. D. McNaught, A. Wilkinson, *IUPAC Compendium of Chemical Terminology*, Blackwell Scientific Publications, Oxford, UK **1997**.
- [63] H. C. Zeng, *Curr. Nanosci.e* **2007**, *3*, 177.
- [64] H. G. Yang, H. C. Zeng, *J. Phys. Chem. B* **2004**, *108*, 3492.
- [65] V. Jakanovi, A. Spasi, D. Uskokovi, *J. Colloid Interface Sci.* **2004**, *278*, 342.
- [66] Y. W. Wang, H. Xu, X. B. Wang, X. Zhang, H. M. Jia, L. Z. Zhang, J. R. Qiu, *J. Phys. Chem. B* **2006**, *110*, 13835.
- [67] A. G. Dong, N. Ren, Y. Tang, Y. J. Wang, Y. H. Zhang, W. M. Hua, Z. Gao, *J. Am. Chem. Soc.* **2003**, *125*, 4976.
- [68] Q. Wang, S. Ito, M. Grätzel, F. Fabregat-Santiago, I. Mora-Seró, J. Bisquert, T. Bessho, H. Imai, *J. Phys. Chem. B* **2006**, *110*, 25210.
- [69] I. G. Yu, Y. J. Kim, H. J. Kim, C. Lee, W. I. Lee, *J. Mater. Chem.* **2011**, *21*, 532.